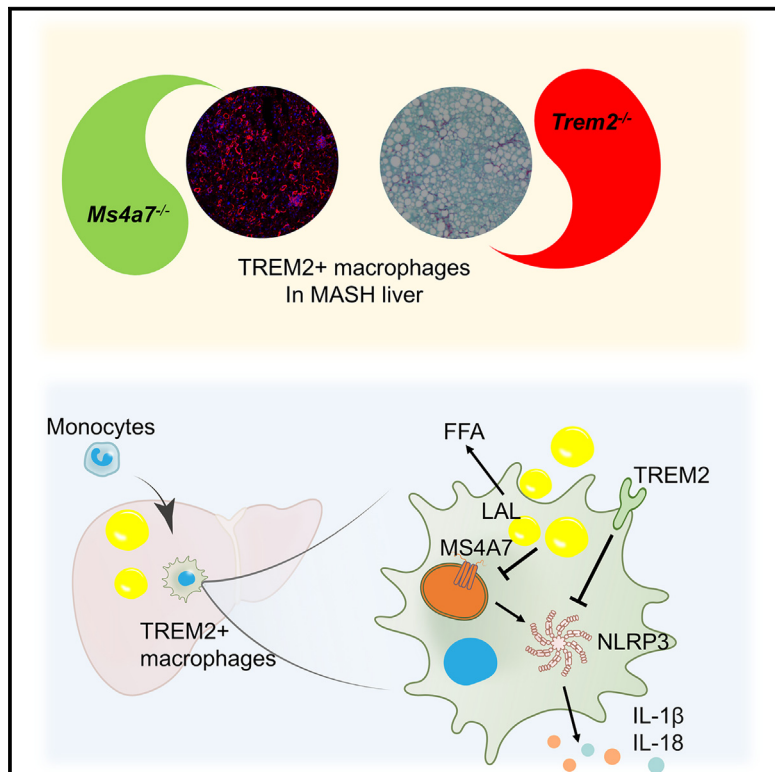


Lipid droplet efferocytosis attenuates proinflammatory signaling in macrophages via TREM2- and MS4A7-dependent mechanisms

Graphical abstract



Authors

Linkang Zhou, You Lu, Xiaoxue Qiu, ..., Hong Du, Siming Li, Jiandie D. Lin

Correspondence

lkzhou@umich.edu (L.Z.), jdlin@umich.edu (J.D.L.)

In brief

Zhou et al. demonstrate that exposure to extracellular LDs triggers a global transcriptional response in macrophages, leading to attenuation of proinflammatory signaling. TREM2 and MS4A7 are dispensable for LD efferocytosis but contribute to its inhibitory effects on macrophage inflammatory response.

Highlights

- LD efferocytosis reprograms global gene expression in cultured macrophages
- Efferocytosed LDs are hydrolyzed by LAL in macrophages
- LD exposure suppresses inflammatory signaling and NLRP3 inflammasome activation in macrophages
- TREM2 and MS4A7 mediate the dampening effects of LD efferocytosis on inflammatory signaling



Article

Lipid droplet efferocytosis attenuates proinflammatory signaling in macrophages via TREM2- and MS4A7-dependent mechanisms

Linkang Zhou,^{1,2,*} You Lu,^{1,2} Xiaoxue Qiu,^{1,2} Zhimin Chen,^{1,2} Yuwei Tang,^{1,2} Ziyi Meng,^{1,2} Cong Yan,³ Hong Du,³ Siming Li,^{1,2} and Jiandie D. Lin^{1,2,4,*}

¹Life Sciences Institute, University of Michigan, Ann Arbor, MI 48109, USA

²Department of Cell & Developmental Biology, University of Michigan Medical Center, Ann Arbor, MI 48109, USA

³Department of Pathology and Laboratory Medicine, Indiana University Simon Cancer Center, Indiana University School of Medicine, Indianapolis, IN 46202, USA

⁴Lead contact

*Correspondence: lkzhou@umich.edu (L.Z.), jdlin@umich.edu (J.D.L.)

<https://doi.org/10.1016/j.celrep.2025.115310>

SUMMARY

Metabolic dysfunction-associated steatohepatitis (MASH) is characterized by injury to steatotic hepatocytes that triggers the release of endogenous danger-associated molecular patterns. Recent work demonstrated that exposed lipid droplets (LDs) serve as a pathogenic signal that promotes monocyte infiltration and its maturation into triggering receptor expressed in myeloid cells 2 (TREM2⁺) macrophages in MASH liver. Here we explore the role of LD exposure in modulating inflammatory signaling in macrophages. We found that LD efferocytosis triggers a global transcriptional response and dampens pro-inflammatory signaling in macrophages. LD treatment attenuated NLRP3 inflammasome activation via mechanisms independent of lysosomal LD hydrolysis. While TREM2 was dispensable for LD efferocytosis by macrophages, it was required for the attenuation of proinflammatory signaling upon LD exposure. Additionally, MS4A7 downregulation contributes to LD efferocytosis-mediated dampening of inflammatory response. These results underscore the dual role of LD exposure in MASH liver by promoting monocyte infiltration and TREM2⁺ macrophage induction, while restraining proinflammatory response in macrophages.

INTRODUCTION

Metabolic dysfunction-associated steatohepatitis (MASH), previously known as non-alcoholic steatohepatitis (NASH), is characterized by stress-induced injury of steatotic hepatocytes, leading to chronic inflammation and liver fibrosis.^{1–4} Damaged hepatocytes release a plethora of intracellular factors and cellular debris that serve as endogenous danger-associated molecular patterns, including ATP, mitochondria, nucleic acids, and certain proteins like HMGB1 and interleukin (IL)-33.^{5,6} Recent work demonstrates that exposure to extracellular lipid droplets (LDs) resulting from steatotic hepatocyte injury promotes monocyte infiltration into the liver and exacerbates liver damage during MASH.⁷ Prolonged LD exposure in mice enhances the induction of hepatic macrophages expressing triggering receptor expressed in myeloid cells 2 (TREM2), highlighting the role of LDs as MASH-associated danger signals that shape the liver immune microenvironment and influences disease progression. Despite this, the nature of LD-mediated danger signaling and its impact on inflammatory signaling in macrophages remain to be elucidated.

Macrophage exhibits distinct polarization states, previously referred to as proinflammatory (M1) and anti-inflammatory (M2)

subtypes. However, this binary M1/M2 framework does not accurately reflect the transcriptomic and functional heterogeneity of macrophages *in vivo*. Single-cell RNA sequencing (scRNA-seq) analyses reveal a spectrum of macrophage populations during MASH, highlighting their heterogeneity.^{8,9} Recent scRNA-seq studies have identified TREM2⁺ macrophages (and microglia) as a common feature of tissue injury and disease pathogenesis. Microglia expressing high levels of TREM2 contribute to the clearance of amyloid plaques in Alzheimer disease.^{10–12} Within the liver, TREM2⁺ macrophages have been observed following diet-induced MASH in mice and in cirrhotic human livers, and as such, were named NASH-associated macrophages and scar-associated macrophages, respectively.^{8,9,13,14} TREM2⁺ macrophages have been observed in adipose tissue during obesity (lipid-associated macrophages), tumorigenesis (tumor-associated macrophages), and atherosclerotic lesions.^{15–18} To simplify nomenclature, we will use TREM2⁺ macrophages to describe this unique population of macrophages hereafter. TREM2⁺ macrophages express a set of unique molecular markers, including TREM2, glycoprotein Nmb (GPNMB), and membrane-spanning 4-domains subfamily A member 7 (MS4A7), and display a transcriptomic signature associated with macrophage phagocytosis, lysosomal degradation, antigen



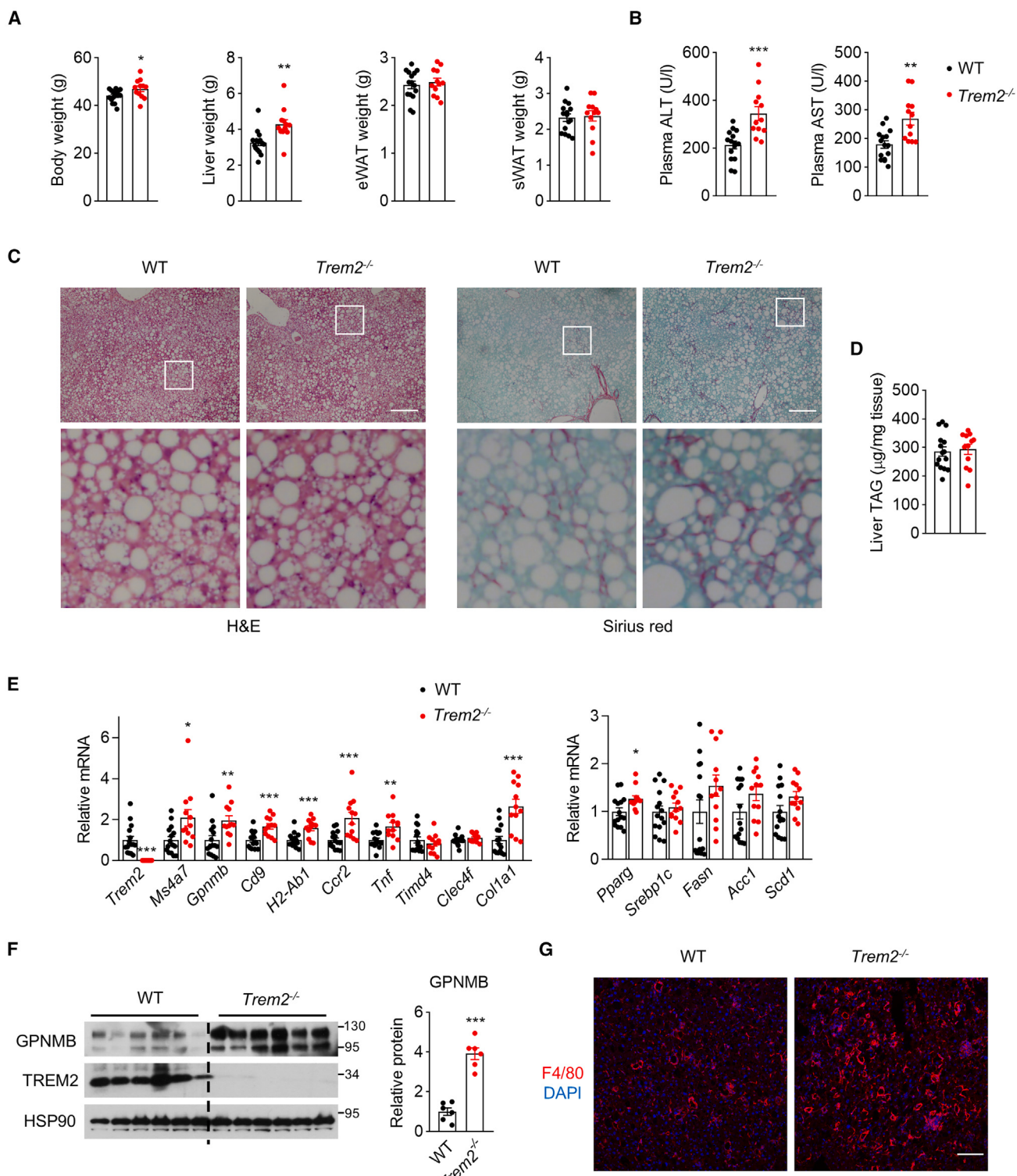


Figure 1. Trem2 ablation exacerbates diet-induced MASH

Control WT ($n = 15$) and Trem2^{-/-} ($n = 12$) male mice were fed a MASH diet for 22 weeks, starting at 10–12 weeks of age.

(A) Body weight and tissue weight.

(B) Plasma ALT and AST concentrations.

(C) Hematoxylin and eosin (H&E) and Sirius red staining of liver sections. Scale bar, 200 μm .

(legend continued on next page)

presentation, and extracellular matrix remodeling.⁸ TREM2-deficient mice developed more severe diet-induced MASH, partially attributed to impaired efferocytosis and aberrant exosome release,^{19,20} whereas the adipose tissue hormone neuregulin 4 attenuates the induction of TREM2⁺ macrophages in MASH liver and suppresses MASH-associated hepatocellular carcinoma.²¹ In contrast, genetic inactivation of *Ms4a7* protects mice from developing MASH-associated pathologies by attenuating NLRP3 inflammasome activation,⁷ underscoring the multifaceted role of TREM2⁺ macrophages in metabolic liver disease.

The pathophysiological cues leading to the induction of TREM2⁺ macrophages include endogenous danger signal and immunomodulatory factors such as transforming growth factor- β . Exposed LDs released from injured steatotic hepatocytes promotes monocyte infiltration into the liver and its maturation into macrophages characteristic of TREM2⁺ macrophages.^{7,21} A recent study demonstrated that hepatic stellate cells from MASH liver promote the expression of *Trem2* in cultured macrophages.²² Aberrant NLRP3 inflammasome activation contributes to diet-induced MASH and other metabolic disorders.^{23,24} Transgenic activation of NLRP3 inflammasome promotes the development of diet-induced MASH pathologies, whereas pharmacological and genetic inactivation of NLRP3 elicited protective functions.^{24–27} Despite this, the role of LD exposure in shaping NLRP3 inflammasome activation in macrophages has not been explored. In this study, we explored the molecular and functional aspects of LD-mediated danger signaling in macrophages, demonstrating that LD efferocytosis triggers global transcriptomic remodeling and dampens pro-inflammatory signaling. Additionally, the study reveals the functional involvements of TREM2 and MS4A7 in mediating the inhibitory effects of LD exposure on macrophage inflammatory response.

RESULTS

Trem2 inactivation accelerates diet-induced MASH in mice

The role of TREM2⁺ macrophages in metabolic liver disease pathogenesis remains to be fully elucidated. To assess whether TREM2 directly affects MASH progression, we subjected wild-type (WT) and *Trem2*^{-/-} mice to MASH diet feeding for approximately 5 months before analysis of MASH parameters. While adiposity remained comparable between the two groups, body weight, liver weight, and plasma ALT and AST levels were significantly elevated in *Trem2*^{-/-} mice upon diet-induced MASH (Figures 1A and 1B). Sirius red and hematoxylin and eosin staining indicated that TREM2 deficiency exacerbated the severity of liver fibrosis without altering hepatic steatosis (Figures 1C and 1D). qPCR analysis of hepatic gene expression revealed elevated expression of several marker genes associated with TREM2⁺ macrophages (*Ms4a7*, *Gpnmb*, *Cd9*, and *H2-Ab1*), cytokine signaling (*Tnf* and *Ccr2*), and liver fibrosis (*Col1a1*) (Figure 1E).

Markers of resident macrophages (Kupffer cells), such as *Timd4* and *Clec4f*, remained largely unaffected by TREM2 deficiency. Western blot analysis revealed a significant increase in GPNMB protein levels in TREM2-deficient mice (Figure 1F). Immunofluorescence staining revealed increased abundance of F4/80⁺ macrophages in *Trem2*^{-/-} mouse liver (Figure 1G). In contrast, hepatic expression of genes involved in lipid metabolism was comparable between control and *Trem2*^{-/-} mice. We recently demonstrated that TREM2⁺ macrophages harbor an intrinsic proinflammatory function mediated by MS4A7-dependent NLRP3 inflammasome activation.⁷ Unlike *Trem2* inactivation, MS4A7 deficiency alleviates diet-induced MASH pathologies in mice. These opposing effects of TREM2 and MS4A7 illustrate a multifaceted role of TREM2⁺ macrophages in shaping liver immune response and metabolic liver disease progression.

LD exposure shapes global gene expression in cultured macrophages

LDs are dynamic intracellular organelles crucial for energy storage across various cell types, notably adipocytes and hepatocytes. LDs contain a lipid ester core of triglycerides and cholesterol esters surrounded by a phospholipid monolayer membrane and membrane-associated proteins on the surface.²⁸ Accumulation and expansion of LDs within hepatocytes resulting from excess lipid flux and *de novo* lipogenesis drive the development of hepatic steatosis during MASH. The presence of crown-like structures (CLS) containing exposed LDs and other cellular debris is a characteristic feature of MASH liver pathologies.^{29,30} Stress-induced injury of steatotic hepatocytes leads to the release of intracellular LDs, which are subsequently cleared by phagocytes such as macrophages. Recent work has demonstrated that LD exposure serves as a danger signal within the MASH liver that triggers monocyte infiltration and its maturation into TREM2⁺ macrophages.⁷ However, whether LD efferocytosis directly impinges on macrophage gene expression and inflammatory signaling remains unknown.

To explore how LD exposure regulates macrophage function, we treated cultured bone marrow-derived macrophages (BMDMs) with LDs isolated from steatotic livers of high-fat diet-fed obese mice. The purity of LDs was confirmed by immunoblotting using antibodies specific for different subcellular compartments (Figure S1A). We used an inverted cell culture system to facilitate the exposure of adherent macrophages to floating LDs in culture media. Differentiated macrophages rapidly engulfed LDs and displayed approximately 5–10 LDs per cell within 3 h (Figures 2A and 2B). We performed transcriptomic analysis on BMDMs to assess the effects of LD efferocytosis on global gene expression in macrophages. Cultured macrophages were treated with PBS or LDs for 3 h followed by incubation in media without LDs for additional 8 h and subjected to RNA-seq analysis. Differential gene expression analysis revealed a total of 350 upregulated and 192 downregulated genes

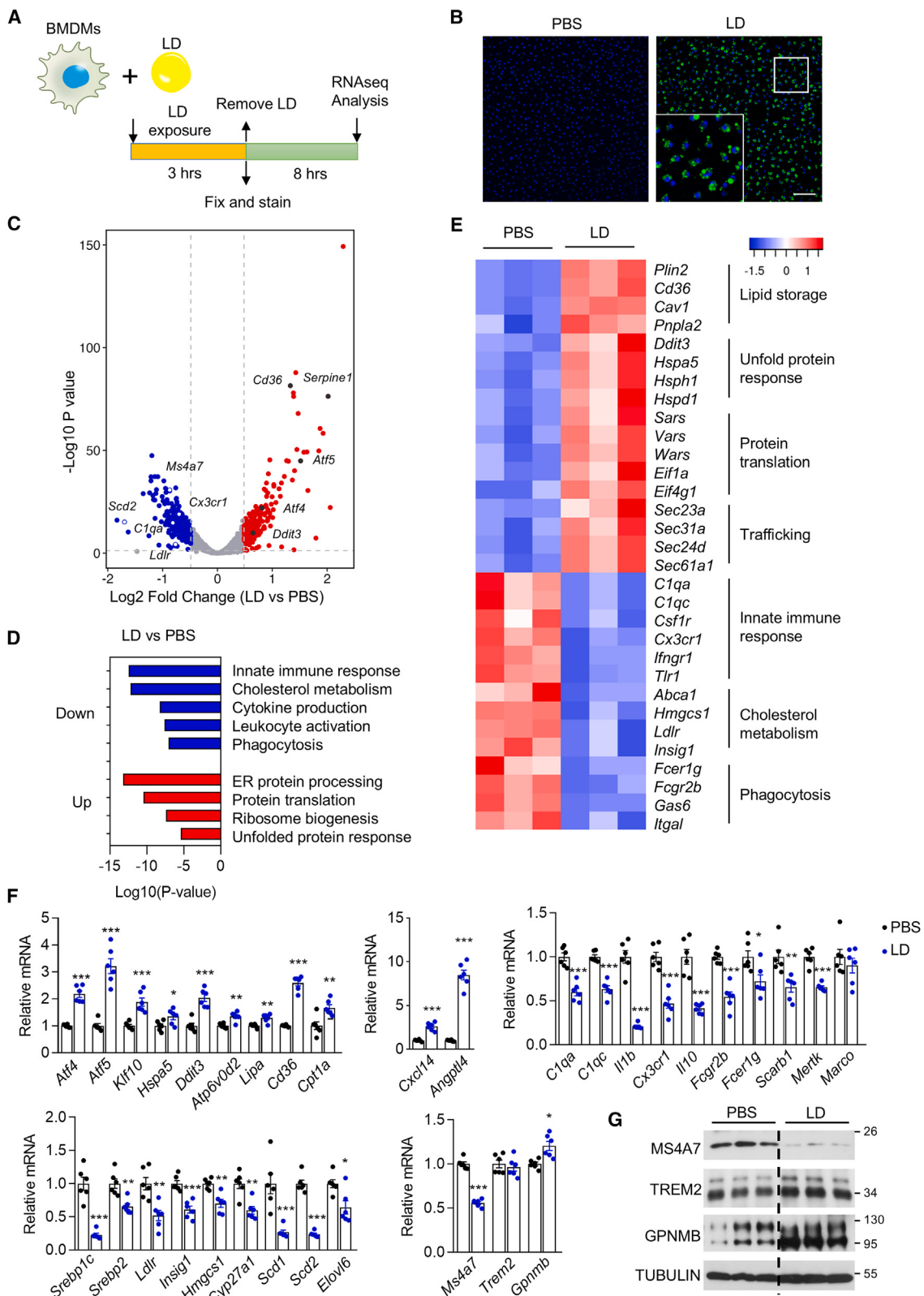
(D) Liver TAG content.

(E) qPCR analysis of hepatic gene expression.

(F) Immunoblots of total liver lysates from WT and *Trem2*^{-/-} mice with quantitation of GPNMB protein levels (right).

(G) F4/80 immunofluorescence staining of liver sections. Scale bar, 100 μ m.

Data represent mean \pm SEM. In all bar graphs, each dot represents one biological replicate. Two-tailed Student t test, * p < 0.05, ** p < 0.01, *** p < 0.001.



(legend on next page)

(1.4-fold) in response to LD treatment (Figure 2C and Table S1). Pathway enrichment analysis revealed that LD-inducible genes were enriched for endoplasmic reticulum protein processing, protein translation, ribosome biogenesis, and unfolded protein response, whereas the downregulated genes were associated with innate immune response, cholesterol metabolism, cytokine production, leukocyte activation, and phagocytosis (Figures 2D and 2E).

qPCR analysis confirmed that LD treatment increased mRNA expression of several genes associated with cellular stress response, including *Ddit3*, *Hspa5*, *Atf4*, *Atf5*, and *Klf10*, lysosomal function (*Atp6v0d2* and *Lipa*), lipid uptake and oxidation (*Cd36* and *Cpt1a*), and secreted factors (*Cxcl14* and *Angptl4*) were also induced in macrophages following LD exposure (Figure 2F). On the contrary, mRNA expression of genes responsible for cholesterol and lipid biosynthesis were decreased by LD treatment, including *Srebp1c*, *Srebp2*, *Insig1*, *Hmgcs1*, *Cyp27a1*, *Scd1*, *Scd2*, and *Elov6*, likely reflecting increased exposure to LD-derived cholesterol. LD treatment also led to decreased mRNA expression of a set of genes involved in immune signaling (*C1qa*, *C1qc*, *Il1b*, *Cx3cr1*, and *Il10*) and pattern recognition (*Fcgr2b*, *Fcer1g*, *Scarb1*, and *Mertk*). Both mRNA and protein levels of MS4A7 were significantly downregulated, whereas TREM2 and GPNMB protein levels were slightly elevated upon LD treatment (Figures 2G and S4A). We next examined the effects of LD exposure on primary liver macrophages isolated from MASH livers. As shown in Figure S1B, LD exposure triggered a transcriptional response in primary liver macrophages that was similar to that observed in BMDMs. We compared LDs isolated from either HFD- or MASH diet-fed mouse livers in treatment studies. LDs from both dietary groups had similar overall effects on macrophage gene expression (Figure S1C). We integrated this dataset with scRNA-seq data for TREM2⁺ macrophages and TREM2⁻ monocyte-derived liver macrophages (GEO: GSE129516).⁸ This analysis revealed that many LD-inducible genes exhibited enriched expression in TREM2⁺ macrophages, whereas those downregulated by LD treatment showed preferential expression in TREM2⁻ monocyte-derived macrophages (Figure S2 and Table S2). Together, these results indicate that exposure of macrophages to LDs triggered a cell-autonomous transcriptional response that is predicted to alter macrophage lipid metabolism and inflammatory response.

LD-mediated efferocytosis dampens proinflammatory signaling in cultured macrophages

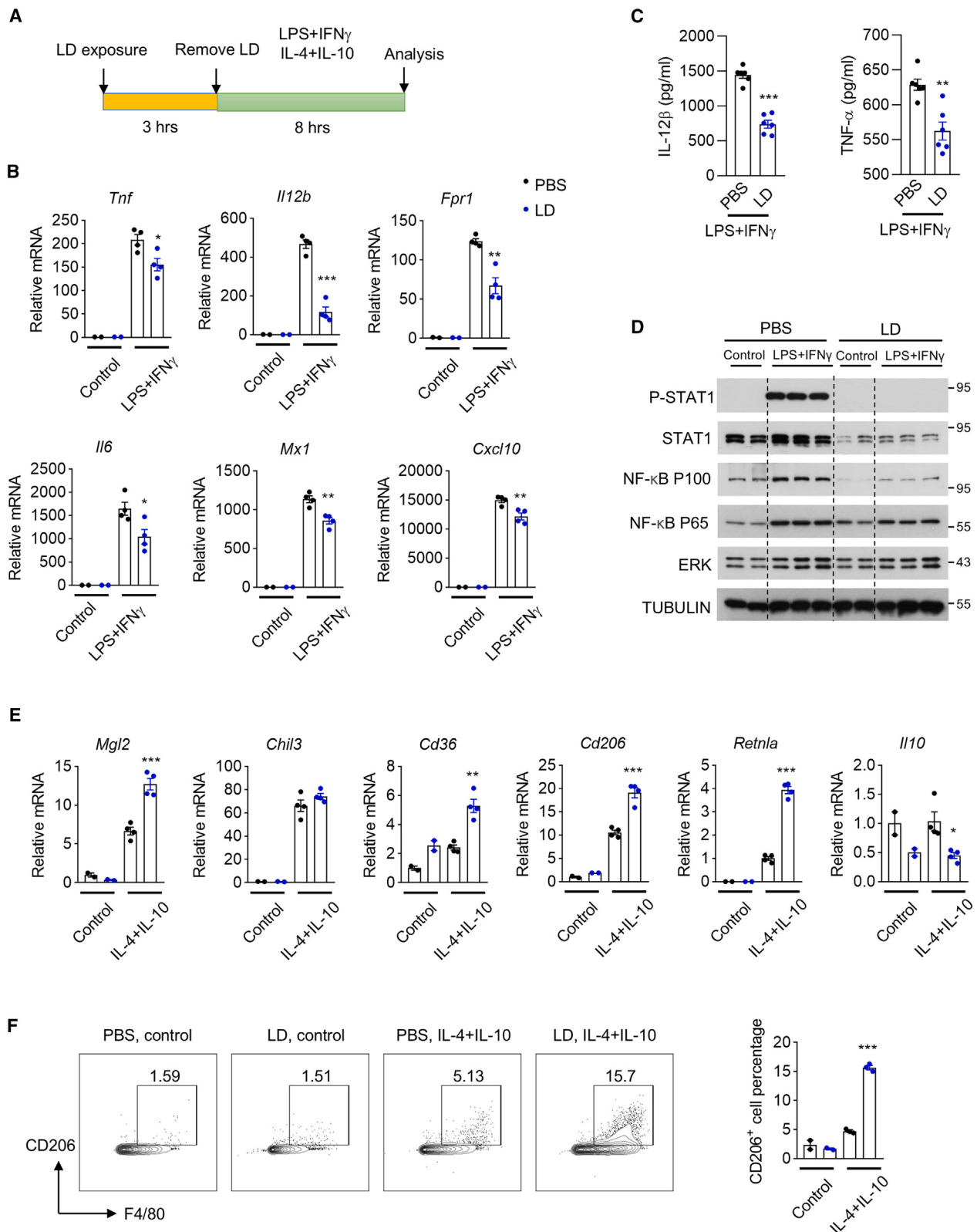
Monocytes recruited to the sites of tissue injury respond to external cues within the tissue microenvironment and undergo

polarization into macrophages with distinct transcriptional and functional characteristics.^{31,32} Under experimental conditions, the combination of lipopolysaccharide (LPS) and interferon γ (IFN- γ) drives proinflammatory macrophage polarization, whereas IL-4 plus IL-10 promote maturation toward macrophages with anti-inflammatory properties. The latter is typically associated with tissue repair, immunomodulation, and resolution of inflammation. To explore how LD exposure modulates inflammatory signaling in macrophages, we treated cultured BMDMs with PBS or LDs for 3 h followed by incubation with LD-free media containing different stimuli (Figure 3A). As expected, LPS + IFN- γ strongly induced mRNA expression of genes involved in inflammatory response, including *Tnf*, *Il12b*, *Ccl2*, *Il1b*, *Fpr1*, *Cxcl10*, *Mx1*, and *Il6* (Figure 3B). Pretreatment of macrophages with LDs significantly diminished the induction of *Tnf*, *Il12b*, *Fpr1*, *Il6*, *Cxcl10*, and *Mx1*, but not *Ccl2* and *Il1b* (Figure S1D), in response to LPS + IFN- γ . Accordingly, IL-12 β and TNF- α release into cultured media were significantly reduced in LD-treated macrophages (Figure 3C). To rule out the potential sequestration of LPS by LDs, we used a cytokine combination of TNF- α and IFN- γ . LD exposure significantly attenuated the induction of *Il12b*, *Il6*, and *Tnf* in response to TNF- α and IFN- γ (Figure S1E). Immunoblotting analysis indicated that NK- κ B and STAT1 protein expression and phosphorylation were markedly decreased by LD exposure (Figures 3D and S4B). The downregulation of the STAT1 pathway strongly correlated with decreased expression of *Cxcl10* and *Mx1*. Treatment with IL-4 and IL-10 stimulated mRNA expression of several genes associated with anti-inflammatory macrophage polarization, including *Mgl2*, *Chil3*, *Cd36*, *Cd206*, and *Retnla*. Interestingly, LD exposure further augmented mRNA expression of these genes except *Chil3* and the induction of CD206⁺ macrophages in BMDM culture (Figures 3E and 3F). Treatment with IL-4 and IL-10 did not enhance *Il10* expression, which was found to be lower in LD-treated BMDMs (Figure 3E).

NLRP3 inflammasome activation is an integral aspect of proinflammatory response elicited by diverse pathogen-derived or endogenous factors.^{26,33} We next examined the effects of LD exposure on NLRP3 inflammasome activation in cultured macrophages (Figure 4A). We treated BMDMs with PBS or LDs followed by LPS priming and ATP stimulation to activate NLRP3 inflammasome. As expected, LPS + ATP treatments markedly activated NLRP3 inflammasome in macrophages, as indicated by a strong increase in IL-1 β cleavage and release into the culture media (Figure 4B and 4C and S4C). LD exposure before LPS + ATP treatments significantly diminished the activation of NLRP3 inflammasome in macrophages, as indicated by

Figure 2. LD exposure shapes global gene expression in cultured macrophages

- (A) Experimental design.
- (B) BODIPY staining of BMDMs treated with PBS or LDs for 3 h. Scale bar, 100 μ m.
- (C) Volcano plot of differentially expressed genes in PBS and LD-treated BMDMs. Blue and red colors denote significantly downregulated and upregulated genes, respectively.
- (D) Gene ontology analysis of genes downregulated (blue) and upregulated (red) in response to LD treatment.
- (E) Heatmap of selected genes regulated by LD treatment.
- (F) qPCR analysis of gene expression in treated macrophages.
- (G) Immunoblots of total BMDM lysates. Data represent mean \pm SEM. In all bar graphs, each dot represents one biological replicate. Two-tailed Student t test, * p < 0.05, ** p < 0.01, *** p < 0.001. See also Figures S1, S2, and S4, and Table S1.



(legend on next page)

reduction in IL-1 β cleavage and release into the culture media. Similar results were obtained using cultured primary liver macrophages isolated from mice with diet-induced MASH (Figures 4D and 4E). We next incubated mouse primary hepatocytes with control or conditioned media (CM) from BMDMs treated with PBS or LDs following NLRP3 inflammasome activation and performed flow cytometry to assess hepatocyte cell death. As shown in Figures 4F and 4G, LD treatment significantly attenuated the cytotoxic effects of BMDM CM on hepatocytes. These observations suggest that efferocytosis of LDs exerts an inhibitory effect on proinflammatory signaling in macrophages.

Role of lysosomal lipid hydrolysis in mediating the effects of LDs on macrophage gene expression

We next investigated the metabolic fate of efferocytosed LDs in BMDMs. We performed BODIPY neutral lipid staining on macrophages exposed to LDs for 3 h followed by incubation in media without LDs for additional 8 h. As expected, macrophages rapidly accumulated LDs following incubation with LDs. The bulk of intracellular LDs disappeared within 8 h, leading to accumulation of free fatty acids (FFAs) in the culture media (Figures 5A–5C). Lysosomal acid lipase (LAL) plays an important role in lysosomal hydrolysis of triglycerides and cholesterol esters.³⁴ To determine whether LAL is responsible for LD hydrolysis in macrophages, we performed LD treatment studies in cultured WT and *Lal*^{-/-} BMDMs. Compared with controls, *Lal*^{-/-} BMDMs had significantly reduced FFA release and consequently accumulated larger intracellular LDs, as revealed by BODIPY staining (Figures 5B and 5C). Similarly, incubation of LD-loaded macrophages with Lalstat1, a selective inhibitor for LAL, markedly decreased LD hydrolysis and FFA release (Figures S3A–S3C). These results demonstrate that lysosomal hydrolysis plays a major role in the catabolism of LDs following efferocytosis.

To assess whether LAL-mediated lipid hydrolysis contributes to the effects of LD exposure on macrophage gene expression, we performed qPCR analysis on WT and *Lal*^{-/-} BMDMs treated with PBS or LDs for 3 h followed by incubation in media without LDs for additional 8 h. We observed that LAL is required for the induction of a subset of macrophage genes in response to LD treatment, including *Cd36*, *Angptl4*, *Serpine1*, and *Atf4* (Figure 5D). Similarly, downregulation of several genes involved in lipid metabolism (*Srebp2*, *Ldlr*, *Srebp1c*, and *Scd1*) was nearly abrogated in macrophages lacking LAL. The decrease in cholesterol-related genes was consistent with the impact of free cholesterol on SREBP2 activation. *Ms4a7* expression was elevated in *Lal* KO BMDMs under PBS and LD-treated conditions. *Trem2* expression was slightly increased in LD-treated

WT BMDMs and further enhanced in LD-treated *Lal* KO BMDMs (Figure 5D). To our surprise, LAL is largely dispensable for the inhibition of NLRP3 inflammasome activation in response to LD exposure (Figure 5E and 5F and S4D). While baseline IL-1 β cleavage and secretion were slightly elevated in *Lal*^{-/-} BMDMs, LD treatment attenuated inflammasome activation in both WT and *Lal*^{-/-} macrophages. Similarly, Lalstat1 did not significantly affect NLRP3 inflammasome activation in the context of LD exposure (Figures S3D and S3E). These results suggest that lysosomal LAL-mediated hydrolysis of LDs contributes to the transcriptional regulation of a subset of macrophage genes. However, LD hydrolysis is not required for its inhibitory effects on NLRP3 inflammasome activation in cultured macrophages.

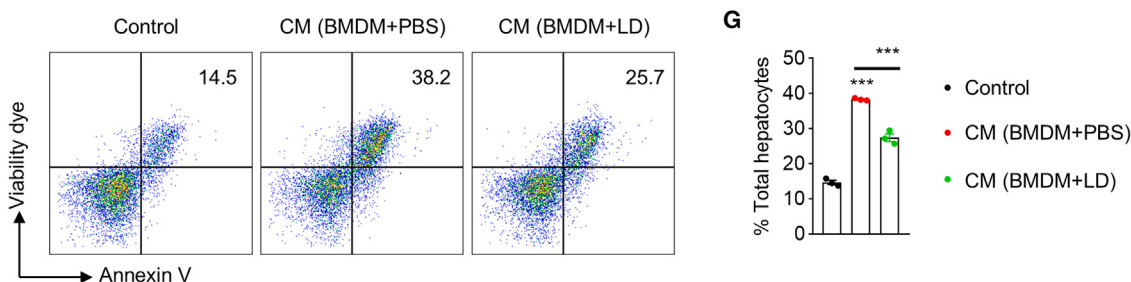
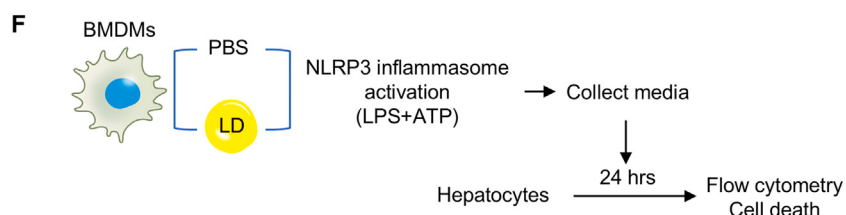
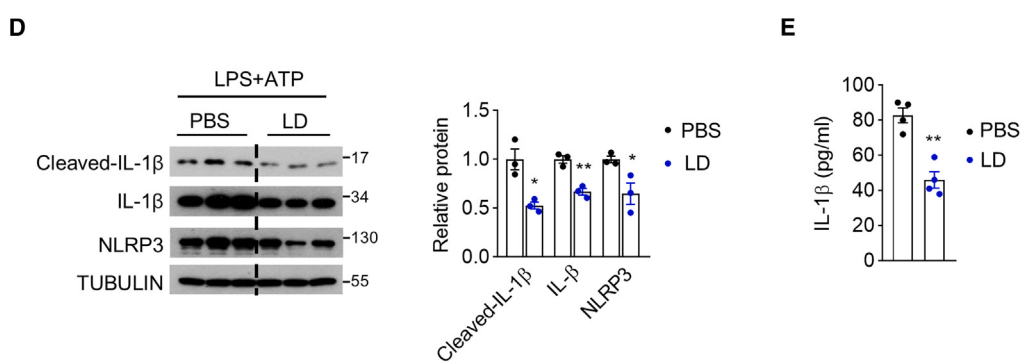
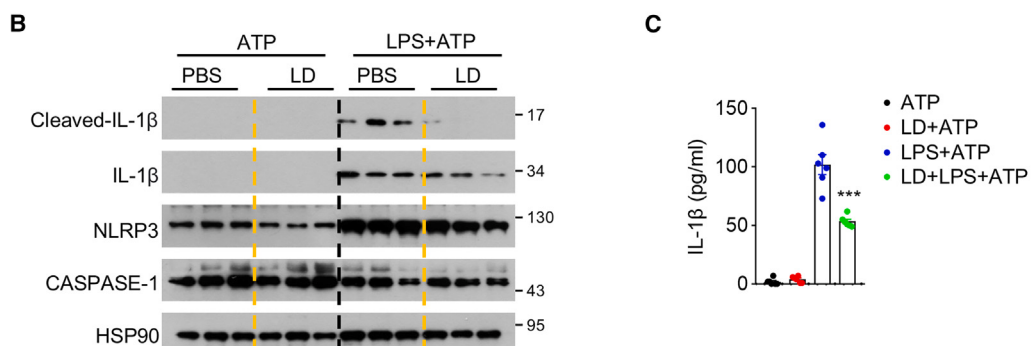
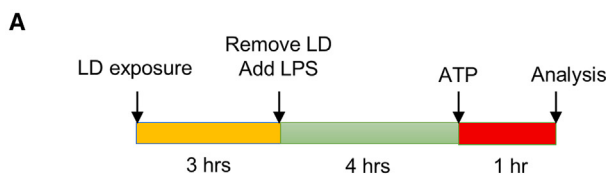
TREM2 is dispensable for LD efferocytosis but required for its dampening effects on proinflammatory signaling

High levels of TREM2 and MS4A7 expression are a prominent feature of TREM2⁺ macrophages in both mouse and human MASH liver.^{7,8} We next explored their role in mediating the suppressive effects of LD exposure on inflammatory signaling in macrophages. We performed NLRP3 inflammasome activation assay on cultured WT and *Trem2*^{-/-} macrophages. Compared with control, macrophages lacking TREM2 displayed elevated IL-1 β cleavage and secretion (Figure 6A, 6B, and S5A). Consistently, immunofluorescence staining with antibodies against ASC (encoded by Pycard), a core component of NLRP3 inflammasome, revealed increased ASC speck formation in *Trem2*^{-/-} macrophages compared with control (Figures 6C and 6D). TREM2 is a cell surface protein that contributes to efferocytosis of various cargos, including protein aggregates and cellular debris.²⁰ To test whether TREM2 is required for LD efferocytosis by macrophages, we incubated WT and *Trem2*^{-/-} BMDMs with isolated LDs and performed BODIPY staining. As shown in Figure 6E, intracellular LD accumulation was comparable between control and *Trem2*^{-/-} macrophages, suggesting that TREM2 *per se* is largely dispensable for LD efferocytosis by macrophages.

We next examined how TREM2 modulates inflammatory signaling in macrophages in combination with LD exposure. We treated WT and *Trem2*^{-/-} macrophages with PBS or LDs before stimulation with a combination of LPS and IFN- γ . As expected, LPS + IFN- γ strongly stimulated mRNA expression of *Fpr1*, *Tnf*, *Il6*, and *Il12b* in treated BMDMs (Figure 6F). Compared with WT control, mRNA induction of *Fpr1* and *Tnf*, but not *Il6* and *Il12b*, was further elevated in *Trem2*^{-/-} macrophages following LPS + IFN- γ stimulation (Figure 6F). LD treatment significantly attenuated the induction of these genes in both genotypes. TREM2 deficiency sensitized macrophages to NLRP3

Figure 3. LD exposure dampens pro-inflammatory signaling in macrophages

- (A) Experimental design. Cultured BMDMs were treated with PBS or LDs for 3 h followed by incubation with LD-free media containing different stimuli for 8 h.
 - (B) qPCR analysis of macrophage gene expression.
 - (C) IL-12 β and TNF- α concentrations in CM.
 - (D) Immunoblots of total macrophage lysates. NF- κ B, nuclear factor κ B.
 - (E) qPCR analysis of macrophage gene expression.
 - (F) Flow cytometry analysis of CD206 expression in BMDMs treated with LDs and IL-4/IL-10.
- Data represent mean \pm SEM. In all bar graphs, each dot represents one biological replicate. Two-tailed Student t test, * p < 0.05, ** p < 0.01, *** p < 0.001. See also Figures S1 and S4.



(legend on next page)

inflammasome activation, as indicated by elevated IL-1 β cleavage and secretion (Figure 6G, 6H, and S5B). While LD treatment markedly reduced IL-1 β cleavage and secretion in WT macrophages, these inhibitory effects on NLRP3 inflammasome activation was significantly diminished in *Trem2*^{-/-} macrophages. Treatment of primary hepatocytes with macrophage CM revealed that hepatocyte cell death was more robustly induced by CM from *Trem2*^{-/-} macrophages than WT control (Figure 6I). These results suggest that TREM2 is required for LD efferocytosis-mediated dampening of macrophage inflammasome activation and cytotoxicity against hepatocytes.

MS4A7 downregulation mediates the attenuation of proinflammatory signaling by LD exposure

We recently demonstrated that MS4A7 promotes NLRP3 inflammasome activation in TREM2⁺ macrophages.⁷ Like TREM2, MS4A7 was not required for efferocytosis of LDs by cultured macrophages (Figure 7A). Consistent with previous findings, MS4A7 ablation attenuated the induction of proinflammatory gene expression in response to LPS + IFN- γ stimulation (Figure 7B). While LD treatment attenuated the induction of these genes in WT macrophages, it failed to elicit further reduction in *Ms4a7*^{-/-} macrophages. Additionally, while both MS4A7 ablation and LD treatment dampened NLRP3 inflammasome activation, LD treatment failed to further attenuate NLRP3 inflammasome activation in MS4A7-deficient macrophages (Figures 7C, 7D, and S5C). Co-immunoprecipitation studies indicated that LD exposure decreased the physical interaction between endogenous MS4A7 and NLRP3 in cultured macrophages (Figure 7E). We next examined the effects of LD treatment and MS4A7 ablation in modulating the cytotoxic effects of macrophages on hepatocytes. We incubated mouse primary hepatocytes with CM from control (no BMDMs), WT, or *Ms4a7*^{-/-} BMDMs following NLRP3 inflammasome activation. Macrophage CM elicited a robust cytotoxic effect on hepatocytes that was attenuated by MS4A7 ablation and LD treatment of cultured macrophage (Figures 7F and 7G). However, LD exposure of MS4A7-deficient BMDMs did not lead to further reduction of cytotoxicity on hepatocytes. These results suggest that MS4A7 downregulation may play a major role in mediating the anti-inflammatory effects of LD efferocytosis on macrophages.

DISCUSSION

LDs are intracellular organelles responsible for energy storage in the form of neutral lipids, such as triglycerides and cholesterol

esters.³⁵ Previous studies have focused on the molecular and cellular biology of LD biogenesis and metabolism and their role in energy metabolism. However, the fate of extracellular LDs released by damaged lipid-laden cells, such as adipocytes and steatotic hepatocytes, and their role in engaging the innate immune system remain largely unexplored. A notable feature of adipose tissue dysfunction in obesity is the emergence of numerous CLSs, which contain LD remnants from injured adipocytes surrounded by clusters of immune cells including macrophages.³⁶ Similarly, hepatic CLS is a pathological feature of diet-induced MASH in mice and human MASH.^{7,30,37} The recruitment of macrophages to these sites of tissue injury strongly suggests that exposed LDs may provide a pathophysiological cue that helps to shape the local immune microenvironment. Interestingly, adipocytes are capable of releasing exosome-sized, lipid-laden vesicles that can be taken up by macrophages.³⁸ As such, efferocytosis of cellular debris by macrophages may play an important role in balancing tissue inflammation, promoting tissue repair, and restoring homeostasis.^{39,40}

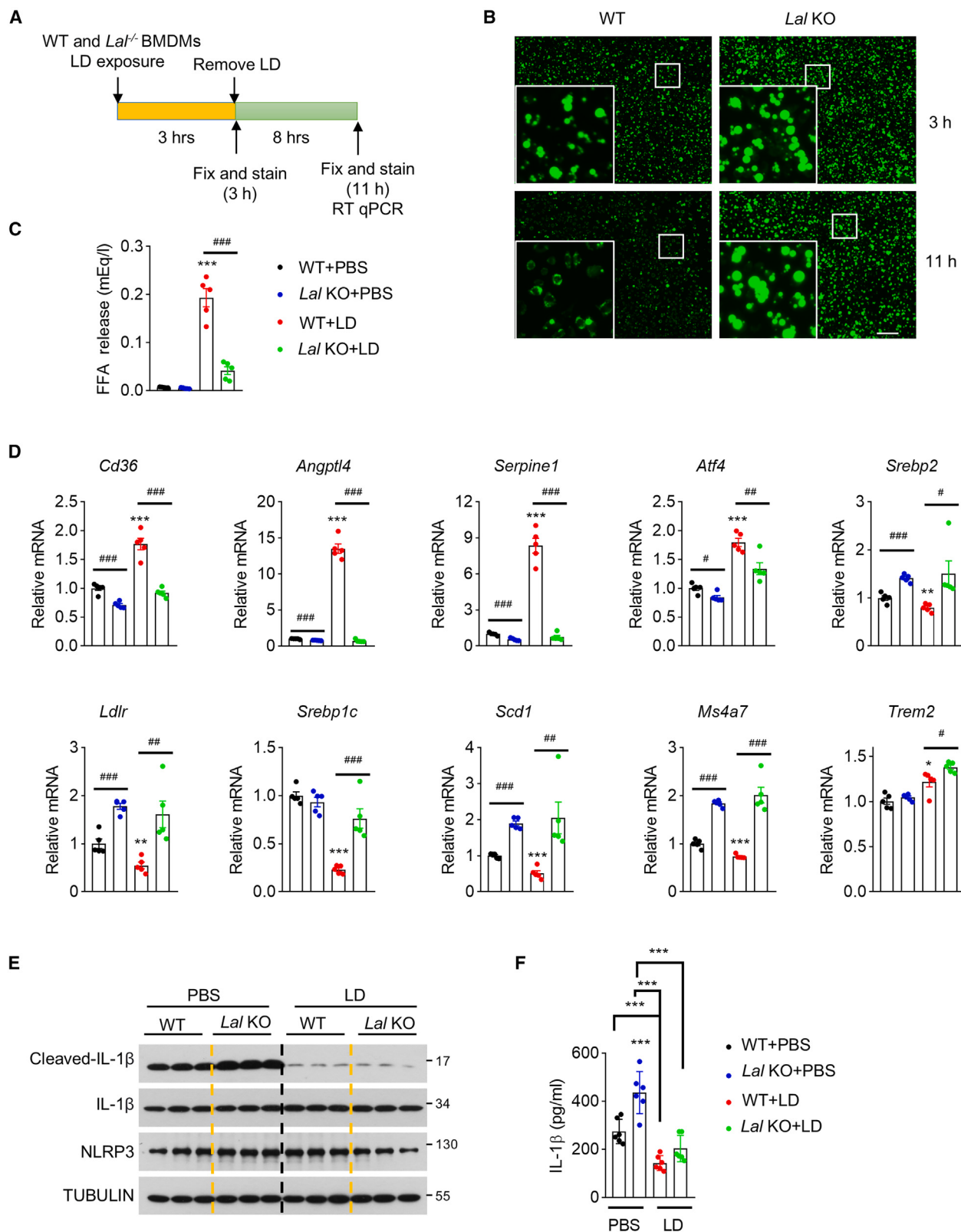
Our recent work demonstrated that LDs serve as a danger signal in MASH liver that triggers monocyte infiltration and its maturation into TREM2⁺ macrophages.⁷ Acute exposure to LDs exacerbated liver injury in mice with diet-induced MASH. Despite this, the pathophysiological effects of LD-mediated danger signaling on macrophage function have not been fully delineated. In this study, we characterized cell-autonomous effects of LD exposure on macrophage gene expression and inflammatory signaling. Cultured macrophages rapidly efferocytosed LDs, which subsequently underwent LAL-dependent lysosomal hydrolysis. Transcriptome analysis revealed that LD treatment elicited robust effects on global gene expression in macrophages, particularly genes involved stress response, innate immune response, and cholesterol metabolism. The exact molecular signals that mediate the transcriptional effects of LDs on macrophages remain unknown. It is possible that LD hydrolysis and metabolism may contribute to the transcriptional landscape of macrophage genes. Alternatively, downstream signaling events triggered by efferocytosis may mediate certain effects of LDs on macrophage gene expression.⁴¹

A somewhat unexpected finding here is that LD efferocytosis robustly attenuates proinflammatory signaling in cultured macrophages in a cell-autonomous manner. LD treatment diminished the stimulatory effects of LPS + IFN- γ on cytokine gene expression and NLRP3 inflammasome activation, leading to reduced cytokine secretion by BMDMs and primary liver

Figure 4. LD exposure attenuates NLRP3 inflammasome activation in macrophages

- (A) Experimental design. Cultured BMDMs were treated with PBS or LDs for 3 h before NLRP3 inflammasome activation using a combination of LPS priming (200 μ g/mL, 4 h) and ATP stimulation (5 mM, 1 h).
- (B) Immunoblots of total cell lysates.
- (C) Concentrations of secreted IL-1 β in culture media ($n = 6$ per group).
- (D and E) NLRP3 inflammasome activation in primary liver macrophages isolated from WT mice fed a MASH diet for 20 weeks. (D) Immunoblots of total cell lysates and quantitation. (E) Concentrations of secreted IL-1 β in culture media.
- (F and G) PBS- and LD-treated BMDMs were subjected to NLRP3 inflammasome activation, and the CM were collected for treatment of cultured primary hepatocytes. Control refers to cells cultured with normal medium. (F) Flow cytometry analysis of hepatocytes using Annexin V and viability dye staining. (G) Quantitation of hepatocyte cell death in (F).

Data represent mean \pm SEM. In all bar graphs, each dot represents one biological replicate. Two-tailed Student t test, * $p < 0.05$, ** $p < 0.01$, *** $p < 0.001$. See also Figure S4.



(legend on next page)

macrophages. These observations suggest that LD exposure likely trigger two phases of macrophage response in the context of MASH liver (Figure 7G). Injury of steatotic hepatocytes and subsequent release of LDs and other danger signals into the extracellular space trigger local inflammatory response characterized by infiltration of innate immune cells including monocytes. A subset of monocytes undergoes transcriptomic and functional polarization into TREM2⁺ macrophages. Prolonged LD exposure and efferocytosis likely promotes further polarization of macrophages toward an anti-inflammatory phenotype, as observed in other settings of macrophage response to efferocytosis.⁴² This dual act of LD-mediated danger signaling may provide an important mechanism for fine-tuning inflammatory response during MASH: LDs released from damaged hepatocytes serve as a danger signal that triggers initial inflammatory response. Prolonged LD exposure and efferocytosis may elicit an anti-inflammatory response, thus facilitating resolution of inflammation and restoration of tissue homeostasis.

Because TREM2⁺ and MS4A7⁺ macrophages were frequently observed adjacent to the CLS in MASH liver,⁷ it is possible that LD exposure may exert its effects on macrophage in part through these two factors. At the functional level, TREM2 is required for the full attenuation of NLRP3 inflammasome activation in cultured macrophages. This is unlikely due to the impairments of efferocytosis in TREM2-deficiency macrophages; we observed comparable activity for efferocytosis of LDs in control and TREM2 null macrophages. Interestingly, LD treatment decreased mRNA and protein expression of MS4A7; the latter promotes inflammatory signaling and NLRP3 inflammasome activation by macrophages. The observations that LD treatment failed to further suppress NLRP3 inflammasome activation in MS4A7-deficient macrophages suggest that its downregulation is likely an important contributor of the anti-inflammatory effects of LD-mediated danger signaling. These results underscore the potentially dichotomous functions of TREM2⁺ macrophages in metabolic liver disease through balancing the pro-inflammatory and anti-inflammatory activities within the evolving liver microenvironment during disease pathogenesis.

Limitations of the study

The current study is focused on delineating the role of LD-mediated danger signaling in shaping macrophage gene expression and inflammatory response. While our experimental results support an anti-inflammatory function of LD exposure in cultured macrophages, several limitations are noted here. First, LD

treatment and functional studies were performed using cultured macrophages. Whether this *in vitro* model fully recapitulates LD-mediated danger signaling in MASH liver microenvironment remains to be confirmed. The molecular signaling pathway that links LD efferocytosis and metabolism to macrophage gene expression and function is not directly addressed in the current study. While TREM2 and MS4A7 partially contribute to the immune-modulatory effects of LDs, the exact biochemical and molecular relationships between these factors and LD signaling in TREM2⁺ macrophages remain to be fully explored. In this study, only male mice were used, which represents a limitation in the research's generalizability. The exclusion of female mice means that potential sex-specific differences in responses or outcomes could not be assessed. Future studies incorporating both male and female mice will be necessary to provide a more comprehensive understanding of the findings and their broader applicability.

RESOURCE AVAILABILITY

Lead contact

Requests for further information, resources, and reagents should be directed to and will be fulfilled by the lead contact, Dr. Jiadie D. Lin (jdlin@umich.edu).

Materials availability

Materials are available from the [lead contact](#) upon reasonable request.

Data and code availability

Raw FASTQ and processed data files from RNA-seq are deposited in the Gene Expression Omnibus (GEO) database (GEO: GSE267716).

This paper does not report any original code.

Any additional information regarding the data can be requested from the [lead contact](#).

ACKNOWLEDGMENTS

We thank Xiaoling Peng for providing technical support; Dr. Regina Feederle at the Monoclonal Antibody Core Facility of Helmholtz Zentrum München, Germany, for sharing the TREM2 antibody; and Dr. Gabriel Nunez at the University of Michigan for sharing the ASC antibody. We thank the University of Michigan Advanced Genomics Core for RNA sequencing data generation. This work was funded by NIH (DK136179 to J.D.L.). L.Z. was supported by the American Heart Association Career Development Award (Award No. 846890).

AUTHOR CONTRIBUTIONS

Conceptualization, J.D.L. and L.Z.; methodology, L.Z. and Y.T.; investigation, L.Z., Z.C., and Z.M.; formal analysis, Y.L., S.L., and X.Q.; writing – original draft, J.D.L. and L.Z.; writing – review & editing, J.D.L. and L.Z.; funding acquisition, J.D.L.; resources, L.Z., J.D.L., C.Y., and H.D.; supervision, J.D.L.

Figure 5. Role of LD hydrolysis in the regulation of macrophage gene expression

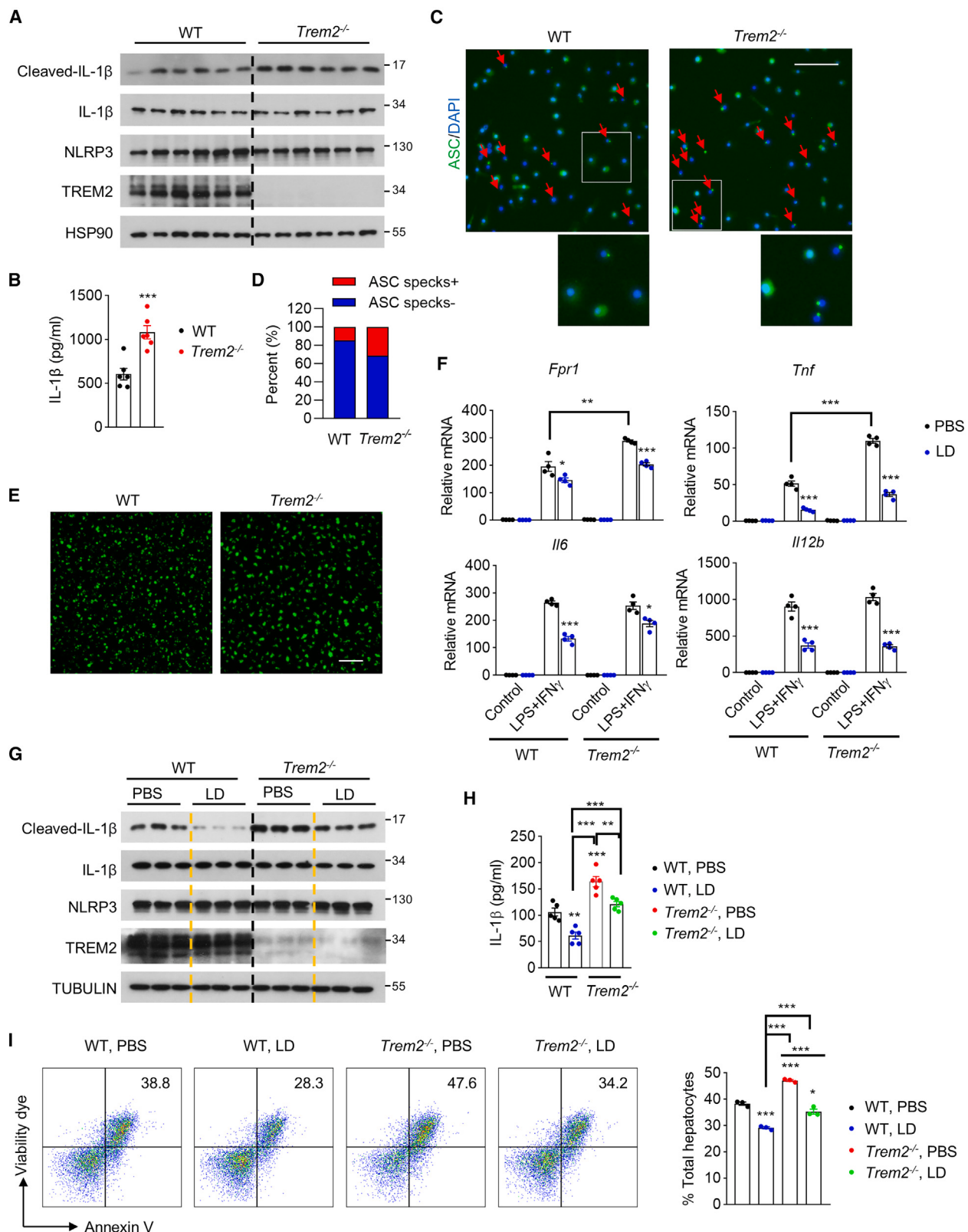
(A) Experimental design.

(B) BODIPY staining. WT and *Lal*^{-/-} BMDMs were incubated with LDs for 3 h and switched to LD-free media for additional 8 h. Scale bar, 100 μm.

(C) Concentrations of FFAs in macrophage culture media following LD treatment. BMDMs were incubated with LDs for 3 h and switched to 3% fatty acid-free BSA dissolved in HBSS for 2 h

(D) qPCR analysis of gene expression.

(E and F) WT and *Lal*^{-/-} BMDMs were loaded with PBS or LDs for 3 h before subjecting to NLRP3 inflammasome activation. (E) Immunoblots of total cell lysates and (F) concentrations of secreted IL-1β in culture media. Data represent mean ± SEM. In all bar graphs, each dot represents one biological replicate. Two-tailed Student t test, * and #p < 0.05, ** and ##p < 0.01, *** and ###p < 0.001. * and # denote the comparison between WT + PBS vs. WT + LD and WT vs. *Lal*^{-/-}, respectively. One-way ANOVA for (F), ***p < 0.001. See also [Figures S3](#) and [S4](#).



(legend on next page)

DECLARATION OF INTERESTS

The authors declare no competing interests.

STAR★METHODS

Detailed methods are provided in the online version of this paper and include the following:

- KEY RESOURCES TABLE
- EXPERIMENTAL MODEL AND STUDY PARTICIPANT DETAILS
 - Animals
 - BMDM isolation and differentiation
 - Primary macrophage isolation
- METHOD DETAILS
 - Liver Triacylglycerol (TAG) analysis
 - LD treatment
 - RNA extraction and qPCR
 - Bulk RNA sequencing
 - Western blot
 - Immunofluorescence staining of cultured macrophages
 - Hepatocyte cell death measurement
- QUANTIFICATION AND STATISTICAL ANALYSIS

SUPPLEMENTAL INFORMATION

Supplemental information can be found online at <https://doi.org/10.1016/j.celrep.2025.115310>.

Received: July 2, 2024

Revised: December 2, 2024

Accepted: January 23, 2025

Published: February 13, 2025

REFERENCES

1. Loomba, R., Friedman, S.L., and Shulman, G.I. (2021). Mechanisms and disease consequences of nonalcoholic fatty liver disease. *Cell* 184, 2537–2564. <https://doi.org/10.1016/j.cell.2021.04.015>.
2. Schwabe, R.F., Tabas, I., and Pajvani, U.B. (2020). Mechanisms of Fibrosis Development in Nonalcoholic Steatohepatitis. *Gastroenterology* 158, 1913–1928. <https://doi.org/10.1053/j.gastro.2019.11.311>.
3. Sheka, A.C., Adeyi, O., Thompson, J., Hameed, B., Crawford, P.A., and Ikramuddin, S. (2020). Nonalcoholic Steatohepatitis: A Review. *JAMA* 323, 1175–1183. <https://doi.org/10.1001/jama.2020.2298>.
4. Suzuki, A., and Diehl, A.M. (2017). Nonalcoholic Steatohepatitis. *Annu. Rev. Med.* 68, 85–98. <https://doi.org/10.1146/annurev-med-051215-031109>.
5. Mihm, S. (2018). Danger-Associated Molecular Patterns (DAMPs): Molecular Triggers for Sterile Inflammation in the Liver. *Int. J. Mol. Sci.* 19, 3104. <https://doi.org/10.3390/ijms19103104>.
6. Park, M.D., Silvin, A., Ginhoux, F., and Merad, M. (2022). Macrophages in health and disease. *Cell* 185, 4259–4279. <https://doi.org/10.1016/j.cell.2022.10.007>.
7. Zhou, L., Qiu, X., Meng, Z., Liu, T., Chen, Z., Zhang, P., Kuang, H., Pan, T., Lu, Y., Qi, L., et al. (2024). Hepatic danger signaling triggers TREM2(+) macrophage induction and drives steatohepatitis via MS4A7-dependent inflammasome activation. *Sci. Transl. Med.* 16, eadk1866. <https://doi.org/10.1126/scitranslmed.adk1866>.
8. Xiong, X., Kuang, H., Ansari, S., Liu, T., Gong, J., Wang, S., Zhao, X.Y., Ji, Y., Li, C., Guo, L., et al. (2019). Landscape of Intercellular Crosstalk in Healthy and NASH Liver Revealed by Single-Cell Secretome Gene Analysis. *Mol. Cell* 75, 644–660.e5. <https://doi.org/10.1016/j.molcel.2019.07.028>.
9. Ramachandran, P., Dobie, R., Wilson-Kanamori, J.R., Dora, E.F., Henderson, B.E.P., Luu, N.T., Portman, J.R., Matchett, K.P., Brice, M., Marwick, J.A., et al. (2019). Resolving the fibrotic niche of human liver cirrhosis at single-cell level. *Nature* 575, 512–518. <https://doi.org/10.1038/s41586-019-1631-3>.
10. Keren-Shaul, H., Spinrad, A., Weiner, A., Matcovitch-Natan, O., Dvir-Szternfeld, R., Ulland, T.K., David, E., Baruch, K., Lara-Astaiso, D., Toth, B., et al. (2017). A Unique Microglia Type Associated with Restricting Development of Alzheimer's Disease. *Cell* 169, 1276–1290.e17. <https://doi.org/10.1016/j.cell.2017.06.030>.
11. Ulland, T.K., and Colonna, M. (2018). TREM2 - a key player in microglial biology and Alzheimer disease. *Nat. Rev. Neurol.* 14, 667–675. <https://doi.org/10.1038/s41583-018-0072-1>.
12. Wang, Y., Cella, M., Mallinson, K., Ulrich, J.D., Young, K.L., Robinette, M.L., Gilfillan, S., Krishnan, G.M., Sudhakar, S., Zinselmeyer, B.H., et al. (2015). TREM2 lipid sensing sustains the microglial response in an Alzheimer's disease model. *Cell* 160, 1061–1071. <https://doi.org/10.1016/j.cell.2015.01.030>.
13. Daemen, S., Gainullina, A., Kalugotla, G., He, L., Chan, M.M., Beals, J.W., Liss, K.H., Klein, S., Feldstein, A.E., Finck, B.N., et al. (2021). Dynamic Shifts in the Composition of Resident and Recruited Macrophages Influence Tissue Remodeling in NASH. *Cell Rep.* 34, 108626. <https://doi.org/10.1016/j.celrep.2020.108626>.
14. Seidman, J.S., Troutman, T.D., Sakai, M., Gola, A., Spann, N.J., Bennett, H., Bruni, C.M., Ouyang, Z., Li, R.Z., Sun, X., et al. (2020). Niche-Specific Reprogramming of Epigenetic Landscapes Drives Myeloid Cell Diversity in Nonalcoholic Steatohepatitis. *Immunity* 52, 1057–1074.e7. <https://doi.org/10.1016/j.immuni.2020.04.001>.
15. Colonna, M. (2023). The biology of TREM receptors. *Nat. Rev. Immunol.* 23, 580–594. <https://doi.org/10.1038/s41577-023-00837-1>.
16. Jaitin, D.A., Adlung, L., Thaiss, C.A., Weiner, A., Li, B., Descamps, H., Lundgren, P., Bleriot, C., Liu, Z., Deczkowska, A., et al. (2019). Lipid-Associated Macrophages Control Metabolic Homeostasis in a Trem2-Dependent Manner. *Cell* 178, 686–698.e14. <https://doi.org/10.1016/j.cell.2019.05.054>.
17. Khantakova, D., Brioschi, S., and Molgora, M. (2022). Exploring the Impact of TREM2 in Tumor-Associated Macrophages. *Vaccines (Basel)* 10, 943. <https://doi.org/10.3390/vaccines10060943>.

Figure 6. Role of TREM2 in mediating the effects of LDs on inflammatory signaling

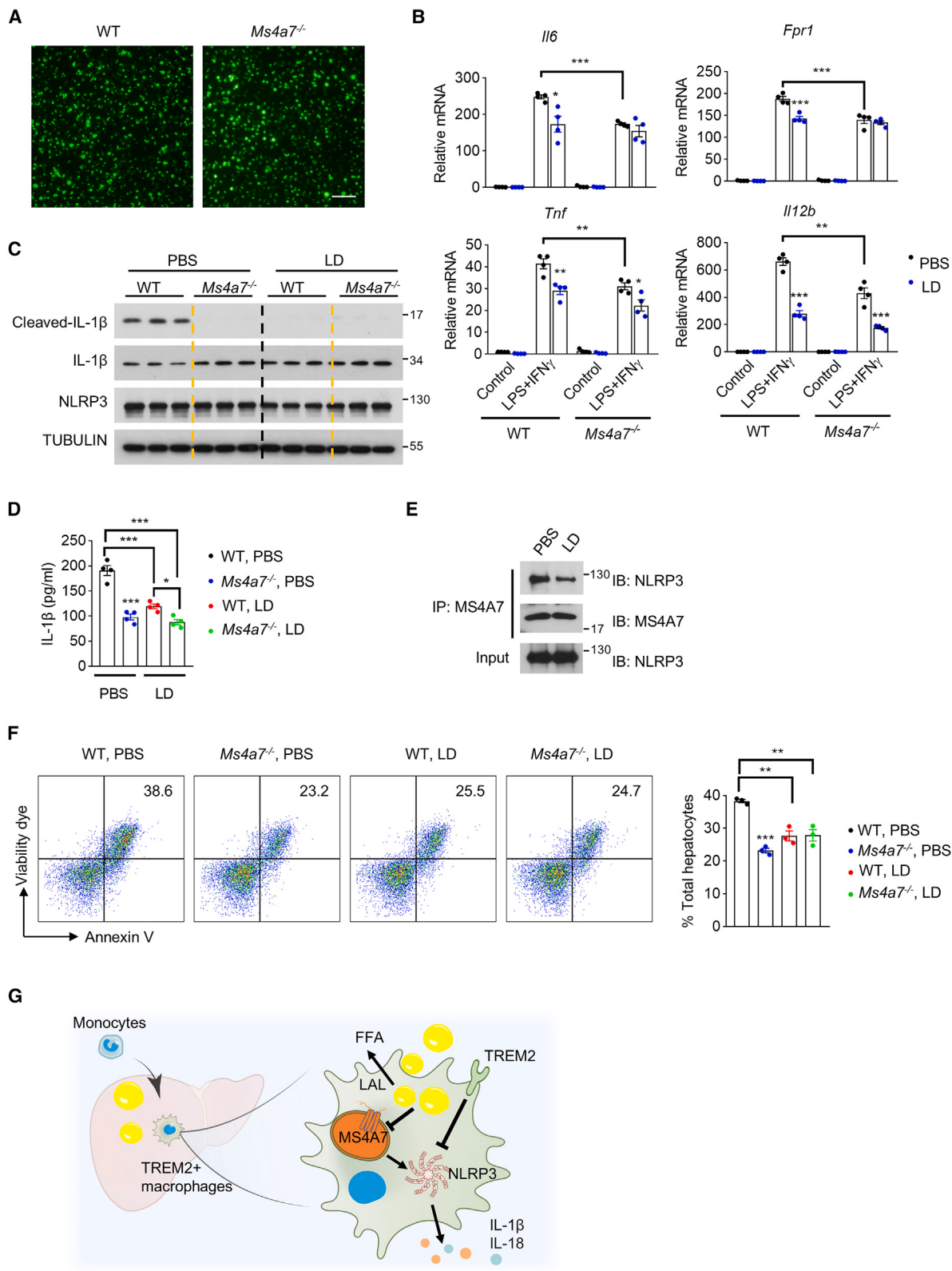
(A–D) WT and *Trem2*^{-/-} BMDMs were subjected to NLRP3 inflammasome activation by exposure to LPS (200 µg/mL) for 4 h, followed by 5 mM ATP treatment for 1 h. (A) Immunoblots of total cell lysates, (B) Concentrations of IL-1β in culture media. (C) ASC immunofluorescence staining. Scale bar, 100 µm. (D) Quantitation of ASC specks (arrowheads) cells.

(E) BODIPY staining of WT and *Trem2*^{-/-} BMDMs treated with LDs for 3 h

(F) WT and *Trem2*^{-/-} BMDMs were treated with PBS or LD for 3 h, followed by LPS (20 ng/mL) and INF-γ (10 ng/mL) for 8 h qPCR analysis of macrophage gene expression.

(G and H) WT and *Trem2*^{-/-} BMDMs were treated with LDs for 3 h and then subjected to NLRP3 inflammasome activation. (G) Immunoblots of total cell lysates, and (H) concentrations of IL-1β in culture media.

(I) Flow cytometry analysis of hepatocyte cell death. WT and *Trem2*^{-/-} BMDMs were treated with PBS or LDs for 3 h and subjected to NLRP3 inflammasome activation. CM were collected for incubation with cultured primary hepatocytes. Data represent mean ± SEM. In all bar graphs, each dot represents one biological replicate. Two-tailed Student t test for (B and F). One-way ANOVA for (H and I). *p < 0.05, **p < 0.01, ***p < 0.001. See also Figure S5.



(legend on next page)

18. Xu, R., Vujic, N., Bianco, V., Reinisch, I., Kratky, D., Krstic, J., and Prokesch, A. (2024). Lipid-associated macrophages between aggravation and alleviation of metabolic diseases. *Trends Endocrinol Metab.* 35, 981–995. <https://doi.org/10.1016/j.tem.2024.04.009>.
19. Hou, J., Zhang, J., Cui, P., Zhou, Y., Liu, C., Wu, X., Ji, Y., Wang, S., Cheng, B., Ye, H., et al. (2021). TREM2 sustains macrophage-hepatocyte metabolic coordination in nonalcoholic fatty liver disease and sepsis. *J. Clin. Invest.* 131, e135197. <https://doi.org/10.1172/JCI135197>.
20. Wang, X., He, Q., Zhou, C., Xu, Y., Liu, D., Fujiwara, N., Kubota, N., Click, A., Henderson, P., Vancil, J., et al. (2023). Prolonged hypernutrition impairs TREM2-dependent efferocytosis to license chronic liver inflammation and NASH development. *Immunity* 56, 58–77.e11. <https://doi.org/10.1016/j.immi.2022.11.013>.
21. Zhang, P., Chen, Z., Kuang, H., Liu, T., Zhu, J., Zhou, L., Wang, Q., Xiong, X., Meng, Z., Qiu, X., et al. (2022). Neuregulin 4 suppresses NASH-HCC development by restraining tumor-prone liver microenvironment. *Cell Metab.* 34, 1359–1376.e7. <https://doi.org/10.1016/j.cmet.2022.07.010>.
22. Chan, M.M., He, L., Finck, B.N., Schilling, J.D., and Daemen, S. (2024). Cutting Edge: Hepatic Stellate Cells Drive the Phenotype of Monocyte-derived Macrophages to Regulate Liver Fibrosis in Metabolic Dysfunction-associated Steatohepatitis. *J. Immunol.* 213, 251–256. <https://doi.org/10.4049/jimmunol.2300847>.
23. Henao-Mejia, J., Elinav, E., Jin, C., Hao, L., Mehal, W.Z., Strowig, T., Thaiss, C.A., Kau, A.L., Eisenbarth, S.C., Jurczak, M.J., et al. (2012). Inflammasome-mediated dysbiosis regulates progression of NAFLD and obesity. *Nature* 482, 179–185. <https://doi.org/10.1038/nature10809>.
24. Mridha, A.R., Wree, A., Robertson, A.A.B., Yeh, M.M., Johnson, C.D., Van Rooyen, D.M., Haczeyni, F., Teoh, N.C.H., Savard, C., Ioannou, G.N., et al. (2017). NLRP3 inflammasome blockade reduces liver inflammation and fibrosis in experimental NASH in mice. *J. Hepatol.* 66, 1037–1046. <https://doi.org/10.1016/j.jhep.2017.01.022>.
25. Kaufmann, B., Kui, L., Reca, A., Leszczynska, A., Kim, A.D., Booshehri, L.M., Wree, A., Friess, H., Hartmann, D., Broderick, L., et al. (2022). Cell-specific Deletion of NLRP3 Inflammasome Identifies Myeloid Cells as Key Drivers of Liver Inflammation and Fibrosis in Murine Steatohepatitis. *Cell. Mol. Gastroenterol. Hepatol.* 14, 751–767. <https://doi.org/10.1016/j.jcmgh.2022.06.007>.
26. Knorr, J., Wree, A., Tacke, F., and Feldstein, A.E. (2020). The NLRP3 Inflammasome in Alcoholic and Nonalcoholic Steatohepatitis. *Semin. Liver Dis.* 40, 298–306. <https://doi.org/10.1055/s-0040-1708540>.
27. Wree, A., McGeough, M.D., Peña, C.A., Schlattjan, M., Li, H., Inzaugarat, M.E., Messer, K., Canbay, A., Hoffman, H.M., and Feldstein, A.E. (2014). NLRP3 inflammasome activation is required for fibrosis development in NAFLD. *J. Mol. Med.* 92, 1069–1082. <https://doi.org/10.1007/s00109-014-1170-1>.
28. Gluchowski, N.L., Becuwe, M., Walther, T.C., and Farese, R.V., Jr. (2017). Lipid droplets and liver disease: from basic biology to clinical implications. *Nat. Rev. Gastroenterol. Hepatol.* 14, 343–355. <https://doi.org/10.1038/nrgastro.2017.32>.
29. Itoh, M., Kato, H., Suganami, T., Konuma, K., Marumoto, Y., Terai, S., Sakugawa, H., Kanai, S., Hamaguchi, M., Fukaiishi, T., et al. (2013). Hepatic crown-like structure: a unique histological feature in non-alcoholic steatohepatitis in mice and humans. *PLoS One* 8, e82163. <https://doi.org/10.1371/journal.pone.0082163>.
30. Daemen, S., Gainullina, A., Kalugotla, G., He, L., Chan, M.M., Beals, J.W., Liss, K.H., Klein, S., Feldstein, A.E., Finck, B.N., et al. (2022). Dynamic Shifts in the Composition of Resident and Recruited Macrophages Influence Tissue Remodeling in NASH. *Cell Rep.* 41, 111660. <https://doi.org/10.1016/j.celrep.2022.111660>.
31. Glass, C.K., and Natoli, G. (2016). Molecular control of activation and priming in macrophages. *Nat. Immunol.* 17, 26–33. <https://doi.org/10.1038/ni.3306>.
32. Hammerich, L., and Tacke, F. (2023). Hepatic inflammatory responses in liver fibrosis. *Nat. Rev. Gastroenterol. Hepatol.* 20, 633–646. <https://doi.org/10.1038/s41575-023-00807-x>.
33. de Carvalho Ribeiro, M., and Szabo, G. (2022). Role of the Inflammasome in Liver Disease. *Annu. Rev. Pathol.* 17, 345–365. <https://doi.org/10.1146/annurev-pathmechdis-032521-102529>.
34. Korbelius, M., Kuentzel, K.B., Bradić, I., Vujić, N., and Kratky, D. (2023). Recent insights into lysosomal acid lipase deficiency. *Trends Mol. Med.* 29, 425–438. <https://doi.org/10.1016/j.molmed.2023.03.001>.
35. Walther, T.C., Chung, J., and Farese, R.V., Jr. (2017). Lipid Droplet Biogenesis. *Annu. Rev. Cell Dev. Biol.* 33, 491–510. <https://doi.org/10.1146/annurev-cellbio-100616-060608>.
36. Lumeng, C.N., Bodzin, J.L., and Saltiel, A.R. (2007). Obesity induces a phenotypic switch in adipose tissue macrophage polarization. *J. Clin. Invest.* 117, 175–184. <https://doi.org/10.1172/JCI29881>.
37. Kanamori, Y., Tanaka, M., Itoh, M., Ochi, K., Ito, A., Hidaka, I., Sakaida, I., Ogawa, Y., and Suganami, T. (2021). Iron-rich Kupffer cells exhibit phenotypic changes during the development of liver fibrosis in NASH. *iScience* 24, 102032. <https://doi.org/10.1016/j.isci.2020.102032>.
38. Flaherty, S.E., 3rd, Grjyalva, A., Xu, X., Ables, E., Nomani, A., and Ferrante, A.W., Jr. (2019). A lipase-independent pathway of lipid release and immune modulation by adipocytes. *Science* 363, 989–993. <https://doi.org/10.1126/science.aaw2586>.
39. Ampomah, P.B., Cai, B., Sukka, S.R., Gerlach, B.D., Yurdagul, A., Jr., Wang, X., Kuriakose, G., Darville, L.N.F., Sun, Y., Sidoli, S., et al. (2022). Macrophages use apoptotic cell-derived methionine and DNMT3A during efferocytosis to promote tissue resolution. *Nat. Metab.* 4, 444–457. <https://doi.org/10.1038/s42255-022-00551-7>.
40. Shi, H., Moore, M.P., Wang, X., and Tabas, I. (2024). Efferocytosis in liver disease. *JHEP Rep.* 6, 100960. <https://doi.org/10.1016/j.jhepr.2023.100960>.
41. Elliott, M.R., Koster, K.M., and Murphy, P.S. (2017). Efferocytosis Signaling in the Regulation of Macrophage Inflammatory Responses. *J. Immunol.* 198, 1387–1394. <https://doi.org/10.4049/jimmunol.1601520>.
42. Saas, P., Vetter, M., Maraux, M., Bonnefoy, F., and Perruche, S. (2022). Resolution therapy: Harnessing efferocytic macrophages to trigger the resolution of inflammation. *Front. Immunol.* 13, 1021413. <https://doi.org/10.3389/fimmu.2022.1021413>.

Figure 7. Role of MS4A7 in LD-mediated attenuation of inflammatory signaling

- (A) BODIPY staining of WT and *Ms4a7*^{-/-} BMDMs treated with LDs for 3 h.
 - (B) WT and *Ms4a7*^{-/-} BMDMs were treated with PBS or LDs for 3 h, followed by LPS (20 ng/mL) and INF-γ (10 ng/mL) for 8 h qPCR analysis of macrophage gene expression.
 - (C and D) WT and *Ms4a7*^{-/-} BMDMs were treated with LDs for 3 h and then subjected to NLRP3 inflammasome activation. (C) Immunoblots of total cell lysates, and (D) concentrations of IL-1β in culture media.
 - (E) Co-immunoprecipitation of endogenous MS4A7 and NLRP3 in cultured BMDMs treated with PBS or LDs.
 - (F) Flow cytometry analysis of hepatocyte cell death. WT and *Ms4a7*^{-/-} BMDMs were treated with PBS or LDs for 3 h and subjected to NLRP3 inflammasome activation. CM were collected for incubation with cultured primary hepatocytes.
 - (G) A model depicting the dual role of LD exposure in triggering monocyte infiltration and maturation to TREM2⁺ macrophages and LD efferocytosis-mediated anti-inflammatory response.
- Data represent mean ± SEM. In all bar graphs, each dot represents one biological replicate. Two-tailed Student t test for (B). One-way ANOVA for (D and F). *p < 0.05, **p < 0.01, ***p < 0.001. See also Figure S5.

43. Ding, Y., Zhang, S., Yang, L., Na, H., Zhang, P., Zhang, H., Wang, Y., Chen, Y., Yu, J., Huo, C., et al. (2013). Isolating lipid droplets from multiple species. *Nat. Protoc.* 8, 43–51. <https://doi.org/10.1038/nprot.2012.142>.
44. Dobin, A., Davis, C.A., Schlesinger, F., Drenkow, J., Zaleski, C., Jha, S., Batut, P., Chaisson, M., and Gingeras, T.R. (2013). STAR: ultrafast universal RNA-seq aligner. *Bioinformatics* 29, 15–21. <https://doi.org/10.1093/bioinformatics/bts635>.
45. Liao, Y., Smyth, G.K., and Shi, W. (2014). featureCounts: an efficient general purpose program for assigning sequence reads to genomic features. *Bioinformatics* 30, 923–930. <https://doi.org/10.1093/bioinformatics/btt656>.
46. Love, M.I., Huber, W., and Anders, S. (2014). Moderated estimation of fold change and dispersion for RNA-seq data with DESeq2. *Genome Biol.* 15, 550. <https://doi.org/10.1186/s13059-014-0550-8>.

STAR★METHODS

KEY RESOURCES TABLE

REAGENT or RESOURCE	SOURCE	IDENTIFIER
Antibodies		
NF-κB P100/P52	Cell Signaling Technology	4882; RRID:AB_10695537
STAT1	Cell Signaling Technology	9172; RRID:AB_2198300
P-STAT1	Cell Signaling Technology	9167; RRID:AB_561284
NF-κB P65	Cell Signaling Technology	8242; RRID:AB_10859369
ERK	Cell Signaling Technology	4695; RRID:AB_390779
Cleaved-IL1b	Cell Signaling Technology	63124; RRID:AB_2799639
IL1b	Cell Signaling Technology	31202; RRID:AB_2799001
NLRP3	Cell Signaling Technology	15101; RRID:AB_2722591
CASPASE-1	Cell Signaling Technology	24232; RRID:AB_2890194
MS4A7	Our lab	N/A
TREM2	A gift from Dr. Regina Feederle from Helmholtz Zentrum Munchen	N/A
ASC	A gift from Dr. Gabriel Nunez from the University of Michigan	N/A
GPNMB	R&D systems	AF2330; RRID:AB_2112934
TUBULIN	Sigma-Aldrich	T6199; RRID:AB_477583
GRP94	Santa Cruz	Sc-32249; RRID:AB_627676
CALNEXIN	Sigma-Aldrich	C4731; RRID:AB_476845
PERILIPIN 2	Fitzgerald Industries	20R-Ap002; RRID:AB_1282475
HSP90	Santa Cruz	Sc-13119; RRID:AB_675659
F4/80 (for staining)	Bio-Rad	MCA497G; RRID:AB_872005
Alexa Fluor 594 Goat Anti-Rat	Thermo Fisher Scientific	A11007; RRID:AB_10561522
Alexa Fluor 488 Donkey Anti-Rat	Jackson ImmunoResearch	712545150; RRID:AB_2340683
PE/Cyanine7 anti-mouse F4/80 Antibody	BioLegend	123114; RRID:AB_893478
PE/Cyanine7 Annexin V	BioLegend	640949
PE anti-mouse CD206 (MMR) Antibody	BioLegend	141705; RRID:AB_10896421
Chemicals, peptides, and recombinant proteins		
DAPI	Thermo Fisher Scientific	10236276001
Trizol	Alkali Scientific	TRZ-100
Protease inhibitor cocktail	Roche	11873580001
MMLV reverse transcriptase	Thermo Fisher Scientific	28025021
SYBR	Thermo Fisher Scientific	4368708
Protein Assay Dye Reagent Concentrate	Bio-Rad	5000006
Collagenase type II	Worthington	LS004176
Optiprep	Serumwerk	1893
BODIPY 493/503	Thermo Fisher Scientific	D3922
Lalistat 1	R&D Systems	6098
M-CSF Recombinant Mouse Protein	BioLegend	576406
LPS	Sigma-Aldrich	L3012
ATP	Sigma-Aldrich	A3377
IFN γ Recombinant Mouse Protein	BioLegend	575306
IL-4 Recombinant Mouse Protein	BioLegend	574302
IL-10 Recombinant Mouse Protein	BioLegend	575802
TNF α Recombinant Mouse Protein	BioLegend	575206

(Continued on next page)

Continued

REAGENT or RESOURCE	SOURCE	IDENTIFIER
Live cell dye	Thermo Fisher Scientific	501129035
Picosirius red	Polysciences	24901
Fast green	Sigma-Aldrich	F7252
Viability dye (eFluor 780)	Thermo Fisher Scientific	501129035
Critical commercial assays		
RNA extraction	Thermo Fisher Scientific	12183025
NEFA kit	Wako Pure Chemical Industries	294-63601
ALT kit	TECO Diagnostics	A524-150
AST kit	Thermo Fisher Scientific	TR70121
Triglyceride determination kit	Sigma-Aldrich	TR0100
Deposited data		
RNA seq	GEO database	GSE267716
Experimental models: Organisms/strains		
C57BL/6J	Jackson Laboratory	000664
Trem2 KO mice	Jackson Laboratory	027197
Ms4a7 KO mice	Our lab	N/A
Lal KO mice	Dr. Hong Du Lab, Indiana University	N/A
Oligonucleotides		
See Table S3		N/A
Software and algorithms		
Flow Jo v10		https://www.flowjo.com/
GraphPad Prism 8.0.1		https://www.graphpad.com/features
ImageJ		https://imagej.net/ij/
R		Version 4.2.0
Other		
HFD	Research Diets	D12492
NASH diet	Research Diets	D09100310

EXPERIMENTAL MODEL AND STUDY PARTICIPANT DETAILS

Animals

All animal studies were performed following procedures approved by the Institutional Animal Care & Use Committee at the University of Michigan. Up to five mice were housed per cage. Mice were maintained on a 12-h light-dark cycle with free access to food and water. *Trem2* KO mice were purchased from the Jackson Laboratory (JAX Strain 027197). The experimental cohorts were generated by separately breeding KO and WT mice derived from the original *Trem2* knockout strain. Mice of two genotypes were cohoused whenever possible for the feeding studies. *Ms4a7* KO mice were generated as previously described.⁷ *Lal* KO mice were provided by Dr. Hong Du (Indiana University). To induce MASH, wild-type and *Trem2* KO male mice were switched from chow to a MASH diet containing 40 kcal % fat, 20 kcal% fructose, and 2% cholesterol (Research Diets, Cat: D09100310) at 10–12 weeks of age. Plasma and tissues were harvested after 5 months of MASH diet feeding for further analysis. Plasma alanine transaminase (ALT) concentrations were measured using a kit from TECO Diagnostics (Cat: A524-150). Plasma aspartate transaminase (AST) concentrations were measured using Infinity AST kits from Thermo Fisher Scientific (Cat: TR70121). For histology, liver tissue was fixed in 4% formalin overnight, embedded in paraffin, and sectioned. Liver sections were then stained with H&E. For Sirius red staining, 0.1% Picosirius red (Polysciences, Cat: 24901) plus 0.1% Fast green (Sigma, Cat: F7252) were used. For immunostaining, liver tissue was fixed in 4% polyformaldehyde at 4°C overnight, followed by overnight immersion in 30% sucrose and embedding in OCT for cryosectioning. The sections were dried at room temperature for 10 min and washed with twice PBS. Tissue permeabilization was achieved using 0.4% Triton-100, and 10% horse serum was used for blocking for 1 h. Primary antibodies (F4/80 (Bio-Rad, Cat: MCA497G)) were added and incubated overnight, followed by the addition of secondary antibodies (Alexa Fluor 594 Goat Anti-Rat (Thermo Fisher Scientific, Cat: A11007)) at room temperature for 1 h. Nuclei were stained with DAPI (Thermo Fisher Scientific, Cat: 10236276001) for 10 min. Images were captured using a Leica SP5 confocal microscope.

BMDM isolation and differentiation

Tibia and femur bones were dissected from young male mice aged six to eight weeks. The ends of each bone were cut off, and the bone marrow was expelled into a 15 mL tube using a 27-gauge needle/25 mL syringe filled with PBS. The resulting cell suspension was centrifuged for 5 min at 500g. Red blood cell lysis buffer was added to the cell suspension to lyse red blood cells. Cells were resuspended and cultured in DMEM containing 10% bovine growth serum, 100 µg/mL penicillin, 100 µg/mL streptomycin and 50 ng/mL M-CSF (BioLegend, Cat:576406) for 5–6 days. Cells were scraped with a Cell Lifter (Thermo Fisher Scientific, Cat: 08-100-240), resuspended, and reseeded depending on the experimental design.

Primary macrophage isolation

Two-month-old male mice were fed a MASH diet for an additional 5 months. The mouse livers were perfused with calcium-free Hank's Balanced Salt Solution (HBSS) containing 0.5 mM EDTA and 0.075% sodium bicarbonate (NaHCO_3), followed by sequential perfusion with HBSS containing 5 mM CaCl_2 , 0.075% NaHCO_3 , and 0.2% collagenase type II (Worthington, Cat: LS004176). Dissociated liver cells were centrifuged at 50g for 5 min to remove hepatocytes. The resulting cell suspension was centrifuged at 500g to isolate non-parenchymal cells (NPCs). NPC pellets were resuspended in FACS buffer, mixed 1:1 with 50% Optiprep solution (Serumwerk, Cat: 1893), and overlaid with FACS buffer. The sample was centrifuged at 1500g for 20 min without brakes. The middle layer of floating cells was collected and plated for 2 h to allow macrophage attachment.

METHOD DETAILS**Liver Triacylglycerol (TAG) analysis**

Approximately 100 mg of liver tissue was homogenized in a buffer containing 50 mM Tris-HCl, 5 mM EDTA, 300 mM mannitol, and protease inhibitors (pH 7.5). An aliquot of 200 µL of the homogenate was mixed with 5 µL of 10 M KOH, followed by the addition of 800 µL of a chloroform/methanol (2:1, v/v) mixture. The solution was vortexed vigorously until it turned white, incubated at room temperature for 5 min, and centrifuged at 10,000 × g for 10 min. The bottom layer (300 µL) was transferred to a new tube and mixed with an equal volume of chloroform/methanol/ H_2O (3:48:47, v/v/v). The mixture was vortexed vigorously and centrifuged at 10,000 × g for 10 min. The bottom layer (120 µL) was carefully transferred to a new tube, dried using a vacuum concentrator, and resuspended in the appropriate TAG resuspension buffer (butanol/Triton X-114/methanol, 9:4:2, v/v/v). Triglyceride levels were measured using the Sigma TAG assay kit (Cat: TR0100) following the manufacturer's instructions.

LD treatment

Lipid droplets (LDs) were isolated from the livers of mice fed a high-fat diet for two months (Research Diets, Cat: D12492), using a previously described method.⁴³ Briefly, fresh liver tissues were homogenized using a Dounce homogenizer. The LD fraction was collected from the top layer after centrifugation and washed three times with PBS. The LD suspension was quantified by counting the number of LDs per microliter and adjusted to 1000–2000 LDs/microliter. For *in vitro* LD treatment, macrophages were seeded onto inverted 30 mm dishes with an opening cut on the side. Culture medium containing LDs isolated from steatotic liver (200 µL LD suspension in 50 mL medium) was added through the hole to facilitate contact between floating LDs and macrophages. After 3 h of incubation, cells were fixed and stained with BODIPY 493/503 (Thermo Fisher Scientific, Cat: D3922) for 20 min. For bulk RNA sequencing, BMDMs were treated with LDs for 3 h. Subsequently, the LDs were removed, and the cells were cultured for an additional 8 h before being harvested. RNA extraction was performed using a commercial kit (Thermo Fisher Scientific, Cat: 12183025), and the samples were sent for sequencing.

For Lalstat1 treatment, after 3 h of LD incubation, LDs were removed, and cells were cultured with or without 10 µM Lalstat1 (R&D Systems, Cat: 6098) for 24 h before fixation for BODIPY staining. Cells were harvested for RNA extraction 8 h after LD removal. For the non-esterified fatty acids (NEFAs) release experiment, after 3 h of LD loading, the medium was replaced with HBSS containing 5% fatty acid free BSA, with or without Lalstat1, for 2 h. The medium was collected to measure NEFA levels using a NEFA kit (Wako Pure Chemical Industries, Cat: 294–63601).

For M1/M2 stimulation, BMDMs were treated with LDs for 3 h. After LD removal, cells were treated with either 20 ng/mL LPS (Sigma, Cat: L3012) plus 10 ng/mL IFN γ (BioLegend, Cat: 575306), or 10 ng/mL IL-4 (BioLegend, Cat: 574302) plus 10 ng/mL IL-10 (BioLegend, Cat: 575802) for 8 h. Cells were collected for western blotting and RNA extraction. Cultured media were collected for CCL2, IL-12 β and TNF- α measurement. For flow cytometry, BMDMs were collected and washed once with FACS buffer (PBS with 1% FBS and 1 mM EDTA). Cells were stained with live-cell dye (eFluro 780, Thermo Fisher Scientific, Cat: 501129035), PE/Cyanine7 anti-mouse F4/80 (BioLegend, Cat: 123114) and PE anti-mouse CD206 (MMR) Antibody (BioLegend, Cat: 141705) for 20 min at room temperature. Samples were analyzed using an Attune NXT4 Flow Cytometer at the MCDB research core facility at the University of Michigan. Data were analyzed using FlowJo software.

For NLRP3 activation, 200 ng/mL LPS was added to the medium for 4 h, followed by 5 mM ATP (Sigma, Cat: A3377) for 1 h. Culture media were collected for IL-1 β measurement and total lysates were prepared for western blotting. Cytokine concentrations in the culture media were measured using ELISA at the Cancer Center Immunology Core at the University of Michigan.

RNA extraction and qPCR

Total RNA was extracted from cells or frozen tissue using TRIzol reagent (Alkali Scientific, Cat: TRZ-100). RNA samples were reverse transcribed to generate cDNA using MMLV reverse transcriptase (Thermo Fisher Scientific, Cat: 28025021). Quantitative PCR (qPCR) was performed using SYBR Green PCR Master Mix (Thermo Fisher Scientific, Cat: 4368708) on an ABI Q6 machine. The primers used for qPCR are listed in [Table S3](#).

Bulk RNA sequencing

Bulk RNA sequencing of BMDMs was conducted at the Advanced Genomics Core, University of Michigan. RNA-seq reads were aligned using the STAR aligner (version 2.7.4a)⁴⁴ against the mouse genome assembly release GRCm38.p6 (NCBI) and gene annotation release M25 (GENCODE). Mapped reads for each gene were quantified using the featureCounts function from the Rsubread package (version 2.0.1)⁴⁵ within the R environment (version 4.2.0). Differentially expressed genes between treatments were identified using the DESeq2 package (version 1.30.0).⁴⁶ Genes with an adjusted P-value <0.05 and Log2(FC) > 0.5 or < -0.5 were considered differentially expressed. Pathway analysis was performed using DAVID Bioinformatics Resources. Raw FASTQ and processed data files from RNA sequencing are deposited in the Gene Expression Omnibus (GEO) database (GEO: GSE267716).

We compared the genes responsive to LD treatment with those associated with TREM2⁺ macrophages by integrating our data with a previously published single-cell RNAseq dataset (GEO: GSE129516).⁸ Macrophages were categorized into Kupffer cells, monocyte-derived macrophages (TREM2⁻ MDMs), and TREM2⁺ macrophages. Genes that showed increased expression in LD-treated BMDMs and were enriched in TREM2⁺ macrophages (fold change ≥ 1.5) were depicted in the heatmap. Similarly, genes downregulated by LD treatment and enriched in TrREM2⁻ MDMs (fold change ≤ 0.6) were also shown in the heatmap. The genes are listed in [Table S2](#).

Western blot

Cultured cells were homogenized directly in 1.5-fold SDS loading buffer (prepared by diluting 3-fold SDS loading buffer (5% SDS, 0.02% bromophenol blue, 25% glycerol, 0.1 M Tris-Cl, pH 6.8 and 6% β -mercaptoethanol added before use)), and boiled at 98°C for 30 min. For blotting MS4A7, 4-fold SDS loading buffer (12% SDS, 0.02% bromophenol blue, 30% glycerol, 0.15 M Tris-Cl, pH 6.8 and 6% β -mercaptoethanol added before use) was used, and samples were incubated in a 37°C water bath for 30 min. For immunoblotting, the following antibodies were used: TREM2 (a gift from Dr. Regina Feederle from Helmholtz Zentrum Munchen), TUBULIN (Sigma, Cat: T6199), HSP90 (Santa Cruz, Cat: sc-13119), NF- κ B P65 (Cell Signaling, Cat: 8242), NF- κ B P100/P52 (Cell Signaling, Cat: 4882), STAT1 (Cell Signaling, Cat: 9172), P-STAT1 (Cell Signaling, Cat: 9167), ERK1/2 (Cell Signaling, Cat: 4695), GPNMB (R&D Systems, Cat: AF2330), Cleaved IL1 β , IL1 β , CASPASE1, NLRP3 (Cell Signaling Mouse Reactive Inflammasome Antibody Kit, Cat: 20836). Anti-NLRP3 mouse antibody was sourced from AdipoGen (Cat: AG-20B-0014). For MS4A7 antibody, the antigen peptide CFPKDIIHKREKTGHYTEKEDD was used. The antigen was injected into New Zealand White Rabbits by Pacific Immunology Corp (CA, USA). The antibody was affinity purified before use in western blotting. The ECL system used was the BrightStar Duration HRP Chemiluminescent 2-Component Substrate ECL Kit (Alkali Scientific Inc, Cat: XR92).

Immunofluorescence staining of cultured macrophages

For ASC speck staining, WT and *Trem2*^{-/-} BMDMs were subjected to the NLRP3 inflammasome activation protocol. Cells were fixed with 4% paraformaldehyde and permeabilized using 0.4% Triton X-100. Blocking was carried out with 10% horse serum. ASC speck staining was performed using an ASC antibody (a gift from Dr. Gabriel Nunez from the University of Michigan) and a secondary anti-body (Alexa Fluor 488 Donkey Anti-Rat, Jackson ImmunoResearch, Cat: 712545150).

Hepatocyte cell death measurement

WT and *Ms4a7*^{-/-} BMDMs were subjected to the NLRP3 inflammasome activation protocol. The medium was collected and filtered through a 3 kD column to remove ATP. Cultured primary hepatocytes were treated with conditioned media collected from WT and *Ms4a7*^{-/-} BMDMs. After 24 h, cells were fixed for microscopy and flow cytometry analyses. For flow cytometry, hepatocytes were digested with trypsin and washed with FACS buffer (PBS with 1% FBS and 1 mM EDTA). Approximately 1x10⁶ liver cells were stained with live cell dye (eFluor 780, Thermo Fisher Scientific, Cat: 501129035) and PE/Cyanine7 Annexin V (BioLegend, Cat: 640949) for 20 min. Samples were analyzed using an Attune NXT4 Flow Cytometer at the MCDB research core facility at the University of Michigan. Data analysis was conducted using FlowJo.

QUANTIFICATION AND STATISTICAL ANALYSIS

Results are presented as mean \pm SEM. Statistical analyses were performed using GraphPad Prism Version 8. Significance was established using two-tailed Student's *t* test or one-way analysis of variance (ANOVA) with Tukey's multiple comparisons test ([Figures 5F; 6H and 6I; 7D and 7F](#)). Differences were considered significant at $p < 0.05$. * $p < 0.05$, ** $p < 0.01$, and *** $p < 0.001$.